Anomalous Translational Diffusion: A New Constraint for Models of Molecular Motion Near the Glass Transition Temperature

Chia-Ying Wang and M. D. Ediger*

Department of Chemistry, University of Wisconsin-Madison, 1101 University Avenue, Madison, WI 53706

Received: September 24, 1999; In Final Form: December 20, 1999

A photobleaching technique has been used to measure the translational motion of tetracene in polystyrene near T_g. The intermediate scattering function $S(q,t)$ was observed to become increasingly non-exponential with decreasing temperature. Thus a clear transition from Fickian diffusion to non-Fickian translational motion has been observed. These results support the view that dynamics are spatially heterogeneous in glass-forming materials. A model of translational motion on heterogeneous lattices indicates that the size of the heterogeneous regions is roughly 20 Å. Thus the data presented here place a new constraint on models of molecular motion near T_g.

I. Introduction

It has been shown that dynamics are spatially heterogeneous in molecular and polymeric glass formers at temperatures near their glass transition temperature T_g.[1−7] Recently developed experimental techniques can select subensembles with dynamics slower or faster than the ensemble average and follow their evolution with time.[3−6] NMR studies by Spiess and co-workers show that the length scale of these heterogeneous dynamic domains is about 3nm in poly(vinyl acetate) at $T_g + 10$ K.[8] Translational diffusion at temperatures around T_g is found to be orders of magnitude faster than what would be expected on the basis of homogeneous dynamics.[9−14] Here we show that measurements of translational motion provide further, direct evidence for heterogeneity in the dynamics.

For many glass forming systems, it has been shown that the rotational and translational mobility of a probe molecule can have different temperature dependencies as T_g is approached.[9−14] These observations are schematically illustrated in Figure 1. Here τ_c and τ_T are the average rotational and translational relaxation times and D_T is the translational diffusion coefficient ($D_T \propto \tau_T^{-1}$). These results can be qualitatively explained if a spatial distribution of relaxation times exists.[15,16] In such a system, translational and rotational motions average over the heterogeneity in different ways. The orientation correlation function is a superposition of the orientation relaxation functions for the different regions of the sample. Molecules in more mobile regions reorient quickly and are responsible for the fast initial decay in the correlation function, while molecules in less mobile regions give rise to a long tail in this function. Since the rotational correlation time τ_c is the integral of the correlation function, it weights regions of slower mobility to a greater extent. In contrast, the long time translational diffusion coefficient D_T emphasizes regions of high mobility. Qualitatively, this is similar to a three dimensional network of random resistors; most of the current follows paths of lower than average resistance. If the distribution of local relaxation times broadens as the temperature is lowered towards T_g, then translational motion (D_T and τ_T) will have a weaker temperature dependence than rotational motion (τ_c).

One consequence of the different temperature dependencies of τ_c and D_T is illustrated at the top right of Figure 1. At sufficiently low temperatures, the time required to translate a long distance (τ_T) must become comparable to the average time for molecular rotation (τ_c). This result has previously been reported for tetracene in polystyrene.[12] This convergence of time scales allows an important prediction if we make the reasonable assumption that rotational and translational motion are locally coupled; i.e., regions where molecules translate slowly are also regions of slow reorientation. When τ_T and τ_c are comparable, it must be true that many molecules have translated a great distance (otherwise translational motion would not be observed on long length scales), while many other molecules have not translated at all (otherwise the rotational correlation function would not be a substantial fraction of unity). Under these circumstances, one should expect to observe non-Fickian translational motion. On the other hand, at higher temperatures where τ_T is much longer than τ_c, all molecules have translated

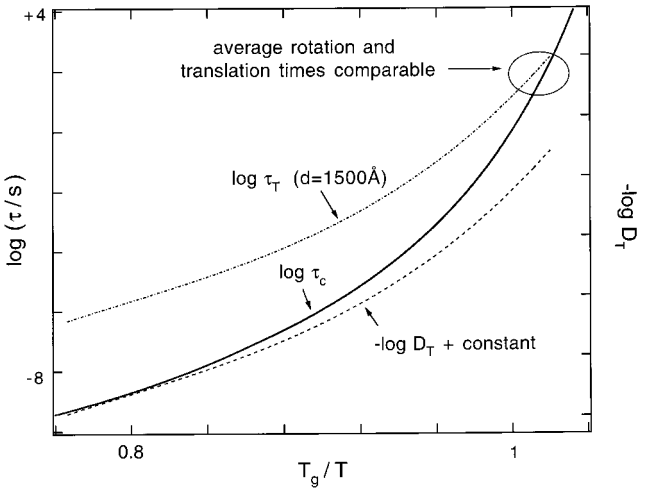

Figure 1. Schematic representation of the different temperature dependencies of rotational and translational motion for probes in supercooled liquids and polymer melts. The translational diffusion coefficient D_T ($\propto \tau_T^{-1}$) has weaker temperature dependence than the rotational correlation time τ_c. As a result, the translational relaxation time τ_T and the rotational correlation time τ_c are approaching each other as the temperature is lowered toward T_g. Note that τ_T is a function of the length scale of the measurement; $d = 1500$ Å for the experiments reported here.

10.1021/jp993420n CCC: $19.00
Published on Web 02/04/2000

some distance before any have translated a long distance. This narrower distribution of translational mobilities is compatible with Fickian diffusion.

Here we report the observation of a transition from Fickian to non-Fickian diffusion for tetracene translation in polystyrene as T_g is approached. In so doing, we expand upon and verify an earlier report of this phenomenon.[12] We have applied a simple model of translational motion on heterogeneous lattices to interpret the experimental data. In this model, random motion on lattices with heterogeneous dynamic domains of either 20 or 80 Å exhibit the same rotational correlation time τ_c and long time translational diffusion coefficient D_T. However, the non-Fickian features of the translational relaxation obtained from simulation of 20 Å heterogeneous regions agree much better with that observed in the experiments than do results for 80 Å domains. As a result, this calculation illustrates that the data presented here place a new constraint on models of molecular motions near T_g.

II. Experimental Section

Sample Preparation. Polystyrene (PS) was purchased from Scientific Polymer Products (M_w = 60 K and M_w/M_n = 1.06). Tetracene (structure shown in Figure 3) was obtained from Aldrich. Samples were prepared by mixing a small amount of tetracene (concentration < 75 ppm) into polystyrene via a freeze−drying method.[12] The tetracene/PS mixture was formed into a 2-mm thick disk using a KBr press. The glass transition temperature, measured by differential scanning calorimetry, is the same for both pure polystyrene and tetracene/polystyrene samples. Using 10 K/min heating/cooling rates and the midpoint convention, $T_g = 373 \pm 2$ K.

Tetracene/polystyrene disks were placed in a 1 cm^2 cuvette filled with silicone oil which served as an index matching fluid and a thermal bath. The silicone oil did not swell the polymer matrix. Samples were held at constant temperature for one day before the measurements were made. All of the data reported here represent dynamics in the *equilibrium* state, since the results do not depend on the length of time that the sample was held at the experimental temperature. Absolute temperatures reported are accurate to ±0.2 K.

Holographic FRAP Technique. The holographic fluorescence recovery after photobleaching (FRAP) technique was used to measure the translational motion of tetracene in polystyrene. A complete description of the FRAP technique can be found in ref 12. Two intense coherent laser beams are crossed in the sample, forming a writing grating. These beams photobleach probes in regions of constructive interference, creating a periodic concentration profile of *unbleached* probes. The grating period d and the grating wavevector q are determined by the angle θ at which the beams intersect:

$$d = \frac{2\pi}{q} = \frac{\lambda}{2\sin(\theta/2)} \qquad (1)$$

Here we use counterpropagating beams ($\theta = 180°$), and λ in the numerator must be replaced by λ/n. Hence, the grating period d is 150 nm (q = 0.042 nm^{-1}) for 476-nm light, considering the polystyrene refractive index n = 1.59. Optical densities of tetracene/PS samples ranged from 0.3 to 0.5 at the tetracene absorption peak of 476 nm. Bleaching times ranged from 0.03 to 0.15 s for bleaching 30% of the probes using 250 mW laser power and a spot size of 1 mm.

Following the photobleaching, a reading grating is formed by attenuating the two intersecting beams. The time dependence of the probe concentration profile can be monitored by measuring the fluorescence intensity as the phase of one reading beam is modulated, causing the reading grating to be swept across the written grating. The modulation of the probe concentration decays with time due to probe translational motion, causing a proportional decrease in the fluorescence modulation. The intermediate scattering function $S(q,t)$ (denoted as $c(q,t)$ in ref 12) is obtained by dividing the amplitude of the fluorescence modulation by the average fluorescence intensity. It is proportional to the spatial Fourier transform of the self part of the van Hove function $G_s(x,t)$[17]:

$$S(q,t)/S(q,0) = \int_{-\infty}^{\infty} G_s(x,t) e^{iqx}\, dx \equiv C(t) \qquad (2)$$

When translational motion is diffusive (or Fickian), $G_s(x,t)$ is Gaussian in space and the translational relaxation function $C(t)$ decays exponentially. For tetracene in polystyrene, translational relaxation was observed to be exponential at T_g+3 K but became non-exponential (non-Fickian) at temperatures below T_g. The non-exponential relaxation functions were fitted with the Kohlrausch−Williams−Watts (KWW) function:

$$C(t) = e^{-(t/\tau_T)^{\beta}} \qquad (3)$$

where τ_T is the translational relaxation time and β characterizes the non-exponentiality of the function. The same values of τ_T and β were obtained whether 30% or 60% of probes were bleached at T = 372.6 K.

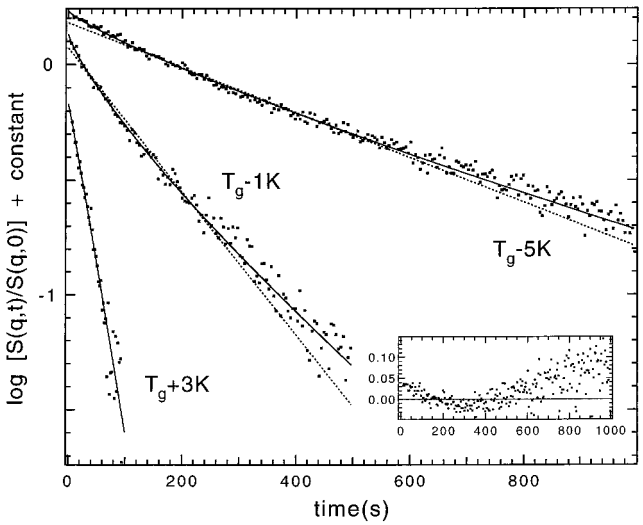

Figure 2. Translational relaxation function $[S(q,t)/S(q,0)]$ at three temperatures for tetracene in polystyrene (q = 0.042 nm^{-1}). Solid line is the best fit of the KWW function and dotted line is the best exponential fit. At T_g + 3 K, an exponential function fits the data well (β = 1). At T_g − 1 K and T_g − 5 K, the KWW function with β = 0.86 and 0.80 fits the data much better. The inset is the residual plot for the exponential fit of the data at T_g − 5 K.

III. Results

Translational mobility measurements on tetracene in polystyrene were performed from 376.2 K ($\approx T_g$ + 3 K) to 367.8 K ($\approx T_g$ − 5 K). Figure 2 shows examples of the intermediate scattering functions obtained in the experiments. At T_g + 3 K, an exponential function fits the data well and β = 1 from the KWW fit. At the two lower temperatures, the KWW function (solid line) fits the data much better than does an exponential function (dotted line). The residual plot for the exponential fit of the data at T_g − 5 K is included as an inset in order to emphasize the deviation from exponentiality. Table 1 lists the

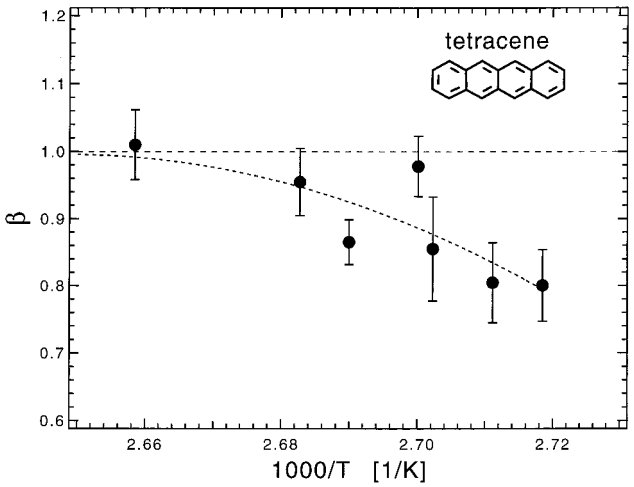

Figure 3. Temperature dependence of the KWW β parameter for translational motion of tetracene in polystyrene ($q = 0.042$ nm^{-1}). The translational relaxation is increasingly non-exponential with decreasing temperature. The structure of tetracene is also shown.

TABLE 1: Values of the Translational Relaxation Time τ_T and the KWW β Parameter for Tetracene in Polystyrene at Temperatures near T_g

temp (K)	τ_T (s)	β
376.2	33±2	1.01±0.05
372.8	107±5	0.95±0.05
371.8	140±10	0.86±0.03
370.4	230±10	0.98±0.04
370.0	240±20	0.85±0.08
368.8	330±20	0.80±0.06
367.8	480±30	0.80±0.05

values of the translational relaxation time τ_T and the β parameter from the best KWW fit of the translational relaxation functions acquired for tetracene in polystyrene; error bars represent 90% confidence intervals based upon 5−10 replicate measurements. The temperature dependence of the KWW β parameter is shown in Figure 3. Translational relaxation becomes increasingly non-exponential with decreasing temperature. The change of the β parameter from 1 to less than 1 represents a transition from Fickian to non-Fickian behavior. As discussed above, all experiments were performed on equilibrium samples so the non-exponential relaxation functions cannot be attributed to non-equilibrium effects such as physical ageing.

IV. Discussion

In the Introduction, we argued that a transition from Fickian to non-Fickian diffusion is expected as the ratio of τ_T/τ_c approaches 1, based on the assumption that dynamics are spatially heterogeneous. Non-Fickian translational motion must be observed when a significant fraction of molecules have not left their starting positions, while another significant fraction have translated many hundreds of Ångstroms. For tetracene in polystyrene, τ_T approaches τ_c in the experimental temperature range (e.g., $\tau_T/\tau_c = 11$ at $T_g + 3$ K and 4 at T_g), and indeed a transition from Fickian to non-Fickian diffusion is observed in Figure 3. Therefore, these results clearly support the view that dynamics are spatially heterogeneous in this system. Due to spatial averaging in the translation measurements (i.e., a grating period of 150 nm is approximately 350 times the tetracene molecular diameter), values of the KWW β parameter for translation ($\beta \geq 0.8$) are greater than those obtained for rotational relaxation ($\beta \sim 0.5$).[18]

We have attempted to quantify the above interpretation with a simulation based on a simple model of translational motion on heterogenous lattices. A complete explanation of this model can be found in ref 16. Translation occurs by nearest-neighbor jumps on a 3D simple cubic lattice which is subdivided into 20 × 20 × 20 cubic blocks. For the cases discussed here, blocks with either 5 or 20 lattice sites along an edge are considered. Translational motion within a given block is homogeneous with a rate controlled by the local rotation time for that block; transitions between different blocks obey microscopic reversibility. The distribution of local rotation times is chosen to be a KWW distribution. The rotation times associated with different blocks are not fixed for all time, but rather exchange on a specified time scale τ_{ex}.

TABLE 2: Parameters for the Heterogeneous Lattice Model[a]

case	τ_c	β	τ_{ex}	block size
I	12	0.37	50	20
II	24	0.31	200	20
III	24	0.31	200	5

[a] $\beta_{ex} = 0.5$ and $\beta_{local} = 0.2$ for all simulations.

Three specific simulations were performed and their parameters are listed in Table 2: the average rotation time τ_c, the width parameter β (denoted as β(sim) in reference 16), and the exchange time τ_{ex}. Trajectories of 1000 independent walks on these heterogeneous lattices were recorded. The self part of the van Hove function $G_s(x,t)$ represents the probability of finding a particle at time t, located x lattice sites away from its original position. Therefore, $G_s(x,t)$ can be directly calculated from these trajectories using multiple starting points. Figure 4 shows the time evolution of the calculated $G_s(x,t)$ for case III. The ordinate is cut off at 0.01 to allow the observation of the broad wings. The spike in the middle of the $G_s(x,t)$ function indicates that a substantial fraction of particles have not moved from their initial position, while others have translated hundreds of lattice sites. As a result, $G_s(x,t)$ is not Gaussian; for comparison, Gaussian curves are also shown in Figure 4 as solid lines. A Gaussian $G_s(x,t)$ was obtained for simulations on a homogeneous lattice where the local rotation times are the same for all blocks.

From these $G_s(x,t)$ functions, the translational relaxation function $C(t)$ {$= [S(q,t)/S(q,0)]$} for a given wavevector q can be calculated by spatial Fourier transform (eq 2). The resulting translational relaxation functions were not always exponential but could be fit with the KWW function (eq 3); thus, each q generates a translational relaxation time τ_T and a β parameter. The relationship between β and the ratio of τ_T/τ_c is exhibited in Figure 5 along with the experimental data. Since the experimental data were acquired at different temperatures, rather than using various q, this is not a completely consistent comparison, but should be qualitatively reasonable. This procedure might account for some of the discrepancy between the simulation results and the experimental data. In the model, one lattice spacing is equal to the diameter of the moving object. Since the hydrodynamic diameter of tetracene is 4.2 Å,[19] a block size of 5 lattice sites corresponds to a domain size of 20 Å and a block size of 20 lattice sites to a domain size of 80 Å.

Figure 5 shows that the model of translational motion on heterogeneous lattices predicts behavior which is qualitatively similar to that observed in the experiments. When the time scale of translational motion approaches that of rotational motion, translational diffusion becomes increasingly non-Fickian. These results support the interpretation that spatially heterogenous dynamics are responsible for the observed non-Fickian diffusion of tetracene in polystyrene. Furthermore, simulation results from a domain size of 20 Å agree much better with the experimental

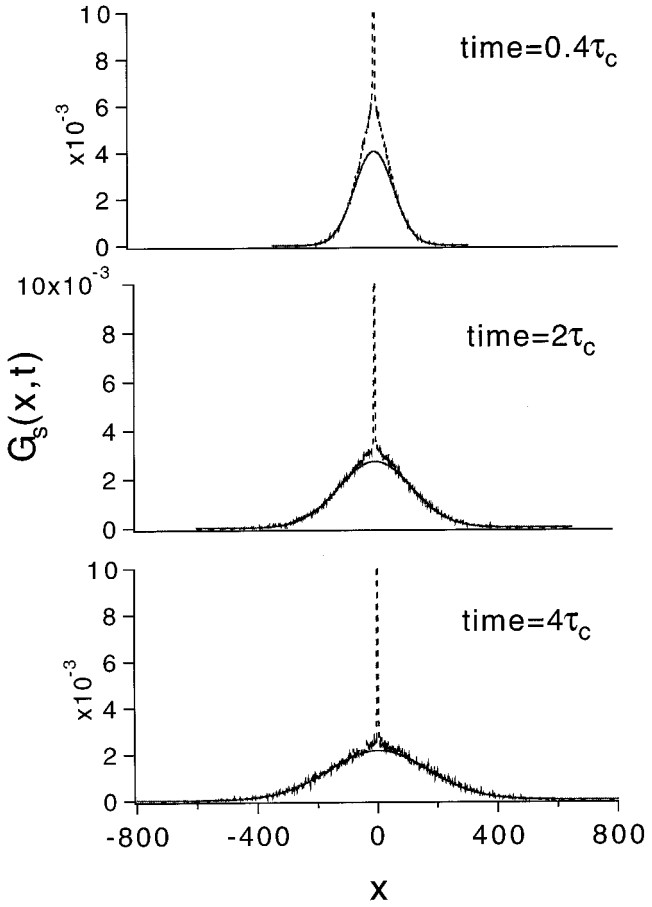

Figure 4. Time evolution of the self part of the van Hove function $G_s(x,t)$ calculated from the heterogeneous lattice model (case III). The ordinate is cut off at 0.01 to allow the observation of the broad wings (the peak is 0.16 at time $t = 0.4\tau_c$ and 0.07, 0.04 at $t = 2\tau_c$, $4\tau_c$, respectively). For example, at time $t = 4\tau_c$, 4% of the particles have not moved from their initial position, while most others have translated hundreds of lattice sites. The solid curve is a Gaussian function and poorly describes $G_s(x,t)$.

observations than the 80 Å domain size. The length scale of 20 Å for domains of heterogeneous dynamics is consistent with NMR measurements[8] on a different polymer near T_g.

An alternative way to examine the transition from Fickian to non-Fickian diffusion would be to investigate the mean-square displacement $<r^2>$, which can be calculated from the simulation trajectories. However, as illustrated in Figure 6, $<r^2>$ is not as sensitive as the intermediate scattering function to the spatially heterogenous dynamics. At a time when the slope of $\log<r^2>$ vs log(time) reaches 1, the intermediate scattering function still shows strongly non-exponential behavior ($\beta < 1$). The inset displays the value of β obtained from the KWW fit of the intermediate scattering function, which is calculated from $G_s(x,t)$ using various q. Each q generates a translational relaxation time τ_T and a β parameter; β values in the main plot are positioned according to the corresponding τ_T value.

The simulations for case II and case III differ only in the domain size. As reported in ref 16, simulations for both cases predict the same rotational correlation time τ_c and long time translational diffusion coefficient D_T within error. However, Figure 5 shows that the length scale of these heterogeneous blocks becomes critical when experimental data on non-Fickian diffusion is available. This illustrates that the data reported here places a new constraint on models of molecular motion near T_g. Other models,[15,20−24] such as the free-energy landscape model developed by Diezemann,[24] should also be capable of

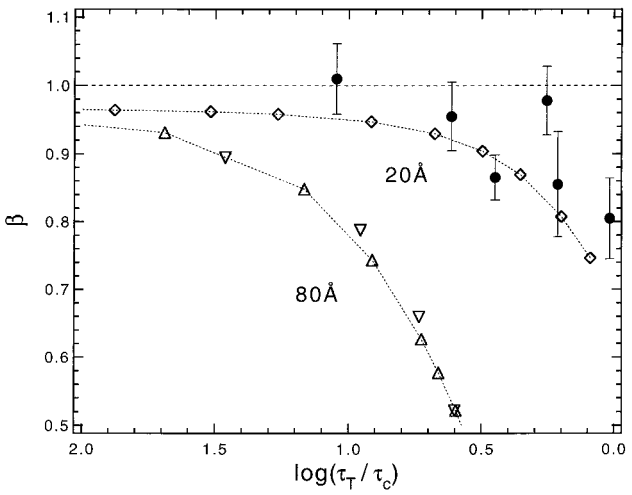

Figure 5. The KWW β parameter of the translational relaxation function vs the ratio of the translational relaxation time τ_T to the rotational correlation time τ_c. Simulation results: case I (triangle), case II (inverse triangle), and case III (diamond). The translational relaxation is increasingly non-exponential as τ_T approaches τ_c for both simulation and experimental data (solid circle). The simulation with heterogenous dynamic domains of 20 Å agrees much better with the experimental data for tetracene in polystyrene than the simulation with 80 Å domains. As described in the text, the abscissa represents changing temperature for the experiment and changing q for the simulation.

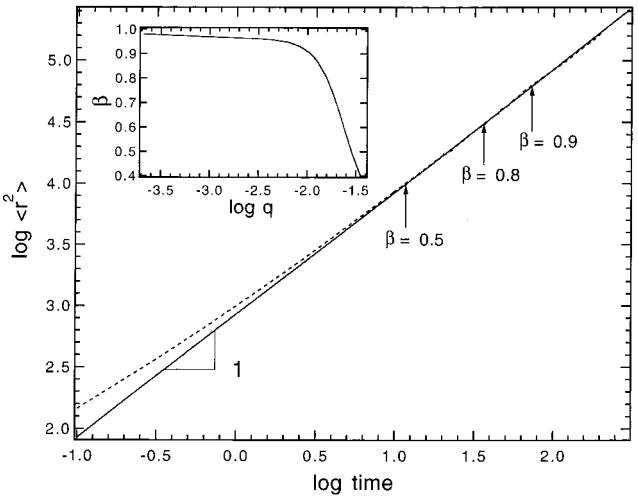

Figure 6. Comparison of the mean-square displacement and the intermediate scattering function as indicators of spatially heterogeneous dynamics. Both quantities are from the simulation trajectories for case III. The mean-square displacement appears to follow Fickian diffusion (slope = 1) at times when the intermediate scattering function still shows non-exponential behavior ($\beta < 1$). Thus the mean-square displacement is less sensitive to spatially heterogenous dynamics than the intermediate scattering function. The inset displays the value of β obtained from the KWW fit of the intermediate scattering function, which is calculated from G_s. The displacement has units of lattice spacings, while 50 time units equal τ_c.

predicting translational relaxation functions. We anticipate that the new results presented here will be useful in discriminating among these various models.

Acknowledgment. We thank Courtney Thompson for the preparation of tetracene/polystyrene samples and the measurements of the glass transition temperature. This work was supported by the National Science Foundation (Grant CHE-9618824).

References and Notes

(1) Moynihan, C. T.; Schroeder, J. *J. Non-Cryst. Solids* **1993**, *160*, 52.

(2) Richert, R. *J. Phys. Chem. B* **1997**, *101*, 6323.

(3) (a) Schmidt-Rohr, K.; Spiess, H. W. *Phys. Rev. Lett.* **1991**, *66*, 3020. (b) Heuer, A.; Wilhelm, M.; Zimmermann, H.; Spiess, H. W. *Phys. Rev. Lett.* **1995**, *75*, 2851.

(4) Bohmer, R.; Hinze, G.; Diezemann, G.; Geil, B.; Sillescu, H. *Europhys. Lett.* **1996**, *36*, 55.

(5) Schiener, B.; Chamberlin, R. V.; Diezemann, G.; Bohmer, R. *J. Chem. Phys.* **1997**, *107*, 7746.

(6) (a) Cicerone, M. T.; Ediger, M. D. *J. Chem. Phys.* **1995**, *103*, 5684. (b) Wang, C.-Y.; Ediger, M. D. *J. Phys. Chem. B* **1999**, *103*, 4177.

(7) Russell, E. V.; Israeloff, N. E.; Walther, L. E.; Gomariz, H. A. *Phys. Rev. Lett.* **1998**, *81*, 1461.

(8) Tracht, U.; Wilhelm, M.; Heuer, A.; Feng, H.; Schmidt-Rohr, K.; Spiess, H. W. *Phys. Rev. Lett.* **1998**, *81*, 2727.

(9) (a) Fujara, F.; Geil, B.; Sillescu, H.; Fleischer, G. *Z. Phys. B* **1992**, *88*, 195. (b) Chang, I.; Fujara, F.; Geil, B.; Heuberger, G.; Mangel, T.; Sillescu, H. *J. Non-Cryst. Solids* **1994**, *172*, 248.

(10) (a) Heuberger, G.; Sillescu, H. *J. Phys. Chem.* **1996**, *100*, 15255. (b) Chang, I.; Sillescu, H. *J. Phys. Chem. B* **1997**, *101*, 8794.

(11) (a) Cicerone, M. T.; Ediger, M. D. *J. Chem. Phys.* **1996**, *104*, 7210. (b) Blackburn, F. R.; Wang, C.-Y.; Ediger, M. D. *J. Phys. Chem.* **1996**, *100*, 18249.

(12) Cicerone, M. T.; Blackburn, F. R.; Ediger, M. D. *Macromolecules* **1995**, *28*, 8224.

(13) (a) Hwang, Y.; Ediger, M. D. *J. Polym. Sci., Polym. Phys. Ed.* **1996**, *34*, 2853. (b) Bainbridge D.; Ediger, M. D. *Rheol. Acta* **1997**, *36*, 209.

(14) Hall, D. B.; Deppe, D. D.; Hamilton, K. E.; Dhinojwala, A.; Torkelson, J. M. *J. Non-Cryst. Solids* **1998**, *235*, 48.

(15) Tarjus, G.; Kivelson, D. *J. Chem. Phys.* **1995**, *103*, 3071.

(16) Cicerone M. T.; Wagner, P. A.; Ediger, M. D. *J. Phys. Chem. B* **1997**, *101*, 8727.

(17) Hansen, J.-P.; McDonald, I. R. *Theory of Simple Liquids*; Academic Press: London, 1986.

(18) (a) Inoue, T.; Cicerone, M. T.; Ediger, M. D. *Macromolecules* **1995**, *28*, 3425. (b) Wang, C.-Y.; Ediger, M. D., *J. Chem. Phys.*, in press.

(19) Cicerone, M. T.; Blackburn, F. R.; Ediger, M. D. *J. Chem. Phys.* **1995**, *102*, 471.

(20) Ngai, K. L.; Rendell, R. W.; Plazek, D. J. *J. Chem. Phys.* **1991**, *94*, 3018.

(21) Stillinger, F. H.; Hodgdon, J. A. *Phys. Rev. E* **1994**, *50*, 2064.

(22) Liu, C. Z.-W.; Oppenheim, I. *Phys. Rev. E* **1996**, *53*, 799.

(23) Perera, D. N.; Harrowell, P. *Phys. Rev. Lett.* **1998**, *81*, 120.

(24) (a) Diezemann, G. *J. Chem. Phys.* **1997**, *107*, 10112. (b) Diezemann, G.; Sillescu, H.; Hinze, G.; Bohmer, R. *Phys. Rev. E* **1998**, *57*, 4398.